EXCLUSIVE REACTIONS AT HERMES

F. ELLINGHAUS*
University of Colorado,
Department of Physics,
Boulder, Colorado 80309-0390, USA
E-mail: Frank.Ellinghaus@desy.de

FOR THE HERMES COLLABORATION

Hard exclusive reactions are the tool to learn about generalized parton distributions, which provide a more complete parameterization of the nucleon than the ordinary parton distribution functions. Measurements performed by the HERMES collaboration of the exclusive production of photons, i.e., Deeply-Virtual Compton Scattering, and of mesons are briefly reviewed, focusing on new results which may allow the determination of the total angular momentum of quarks in the nucleon.

1. Introduction

Similar to the case of inclusive and semi-inclusive DIS, where the nucleon structure is described using **P**arton **D**istribution **F**unctions (PDFs), hard exclusive reactions can be expressed in terms of **G**eneralized **P**arton **D**istributions (GPDs) [1,2,3]. The PDFs and elastic nucleon **F**orm **F**actors (FFs) are included in the GPDs as limiting cases and moments of GPDs, respectively [2]. This is visualized in Fig. 1. While FFs derived in elastic scattering describe the transverse location of partons inside the nucleon and PDFs describe their longitudinal momentum distribution, GPDs are able to provide information on both at the same time. Thus exclusive reactions are able to give a certain 3–dimensional picture of the nucleon structure [4,5,6]. In particular, GPDs offer for the first time a possibility to determine the total angular momentum carried by the quarks in the nucleon [2].

Below the experimental status of measurements on the exclusive production of photons (DVCS) and mesons at HERMES is summarized. The data has been taken with polarized and unpolarized gas targets using the

*This work is supported in part by the US Department of Energy.

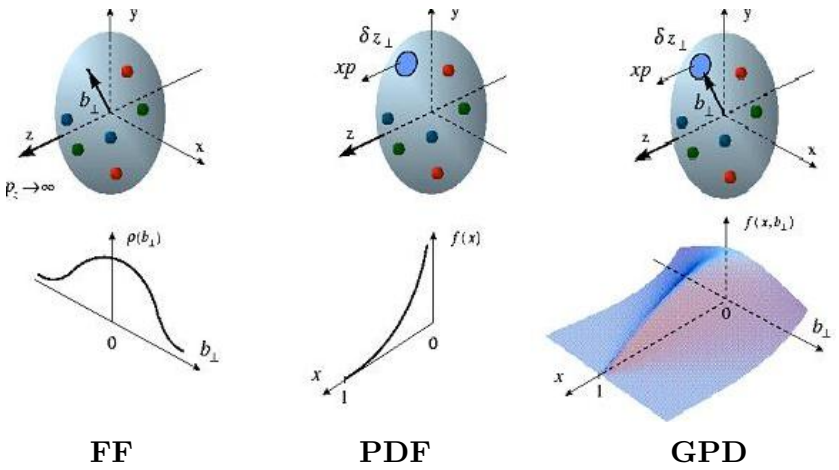

Figure 1. Probabilistic interpretation of form factors (FF), parton distribution functions (PDF) and generalized parton distributions (GPD). For details on figure see Ref. [5].

HERMES spectrometer [7] at the HERA electron/positron–proton collider at DESY, which offers longitudinally polarized 27.6 GeV electron and positron beams. The connection between the measured asymmetries and the four leading twist GPDs H, $\widetilde{H}$, E, $\widetilde{E}$ is given, especially focusing on the connection to the total angular momentum.

2. Deeply–virtual Compton scattering

The hard exclusive leptoproduction of real photons, e.g., $e\,p \to e\,p\,\gamma$, is called **D**eeply–**V**irtual **C**ompton **S**cattering (DVCS). DVCS amplitudes can be measured through the interference between the DVCS and **B**ethe–**H**eitler (BH) processes, in which the photon is radiated from a parton in the former and from the electron in the latter process. Both processes have an identical final state, i.e., they are indistinguishable, and thus their amplitudes (τ_{DVCS}, τ_{BH}) add coherently. For an unpolarized proton target, the cross section for the exclusive leptoproduction of photons reads [8]

$$\frac{d\sigma}{dx_B\,dQ^2\,d|t|\,d\phi} = x_B\,y^2\,\frac{|\tau_{BH}|^2 + |\tau_{DVCS}|^2 + \overbrace{\tau_{DVCS}\,\tau^*_{BH} + \tau^*_{DVCS}\,\tau_{BH}}^{I}}{32\,(2\pi)^4\,Q^4\,\sqrt{1+4\,x_B^2\,M_p^2/Q^2}}, \tag{1}$$

where x_B represents the Bjorken scaling variable, $-Q^2$ the virtual–photon four–momentum squared, y the fraction of the incident lepton energy car-

ried by the virtual photon and t and M_p are the Mandelstam variable and the proton mass, respectively. The azimuthal angle ϕ is defined as the angle between the lepton scattering plane, and the photon production plane made up correspondingly by the virtual and the real photon. At leading twist, the interference term I is given by [8]

$$I = \pm \frac{\sqrt{32}}{t\,Q\,x_B} \frac{m\,e^6}{\sqrt{1-x_B}} \left[\cos\phi \frac{1}{\sqrt{\epsilon(1-\epsilon)}} \mathcal{R}eM^{1,1} - P_l \sin\phi \sqrt{\frac{1+\epsilon}{\epsilon}} \mathcal{I}mM^{1,1} \right], \quad (2)$$

where +(-) denotes a negatively (positively) charged lepton beam with polarization P_l, e represents the electron charge and ϵ is the ratio of the number of longitudinal to transverse initial photons in the DVCS process. The ϕ–dependence of a cross section asymmetry with respect to the charge (spin) of the lepton beam predominantly singles out the $\cos\phi$ ($\sin\phi$) amplitude of the interference term, which provides information about the real (imaginary) part of the DVCS amplitude $M^{1,1}$. The DVCS amplitude [9]

$$M^{1,1} = F_1\,H_1 + \frac{x_B}{2-x_B}(F_1+F_2)\,\tilde{H}_1 - \frac{t}{4M^2}F_2\,E_1 \quad (3)$$

is given by a linear combination of the so–called Compton form factors (CFFs) H_1, $\tilde{H}_1$ and E_1, together with the Dirac and Pauli form factors F_1 and F_2, respectively. The CFFs are convolutions of the respective twist–2 GPD H, $\tilde{H}$ or E and of the hard scattering amplitude. While the above holds true only for an unpolarized target, other linear combinations of GPDs can be accessed in a similar way using a longitudinally or transversely polarized proton target.

The event selection at HERMES requires events with exactly one photon and one charged track, identified as the scattered lepton, with $Q^2 > 1$ GeV^2. The photon is identified by detecting an energy deposition in the preshower scintillator and in the calorimeter without an associated charged track. The recoiling proton is not detected. Exclusive events are identified by the fact that the missing mass of the reaction $ep \to e\gamma X$ corresponds to the proton mass. Due to the finite energy resolution the exclusive sample is defined as $-1.5 < M_x < 1.7$ GeV, as determined from signal–to–background studies using a Monte-Carlo simulation. A recoil detector, presently being assembled in the target area, will help to more clearly identify exclusive reactions and thus to reduce the underlying background to less than 1%.

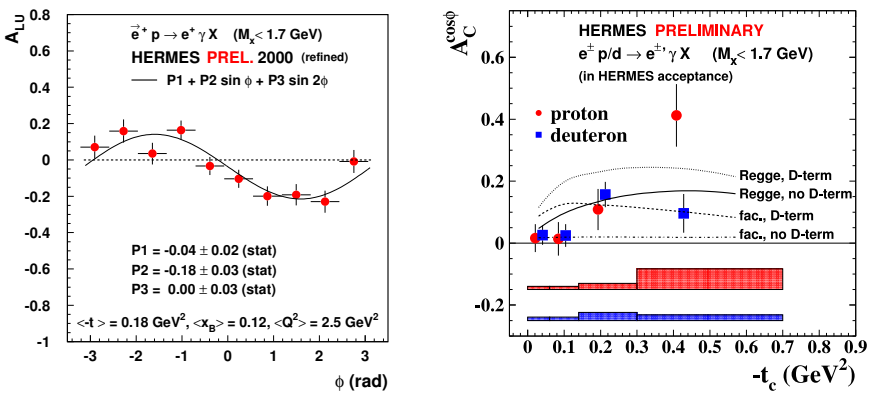

Figure 2. Left panel: Beam–spin asymmetry A_{LU} for the hard electroproduction of photons off the proton [10] as a function of the azimuthal angle ϕ for the exclusive sample. The solid curve shows the result of the indicated fit with the values given in the plot. Right panel: The $\cos\phi$ amplitude of the beam–charge asymmetry on hydrogen and on unpolarized or spin–averaged polarized deuterium [12] as a function of $-t$ at average values of $\langle x_B \rangle = 0.10$ and $\langle Q^2 \rangle = 2.5$ GeV^2. The GPD model calculations use a factorized or a Regge–inspired t–dependence with or without a D-term contribution.

2.1. *Access to GPD H via beam-charge asymmetry, "ordinary (charged)" and "neutral" beam-spin asymmetry*

The beam–spin asymmetry (BSA) and the beam–charge asymmetry (BCA) as a function of ϕ are calculated as

$$A_{LU}(\phi) = \frac{1}{< |P_l| >} \frac{\overrightarrow{N}(\phi) - \overleftarrow{N}(\phi)}{\overrightarrow{N}(\phi) + \overleftarrow{N}(\phi)}, \qquad A_C(\phi) = \frac{N^+(\phi) - N^-(\phi)}{N^+(\phi) + N^-(\phi)}, \quad (4)$$

with the normalized yields $\overrightarrow{N}$ ($\overleftarrow{N}$) or N^+ (N^-) using a beam with positive (negative) helicity or a positron (electron) beam, respectively. The BSA on the proton as a function of ϕ is shown in the left panel of Fig. 2 for the exclusive sample [10]. The results from the indicated fit show the $\sin\phi$ dependence for the BSA as expected from Eqn. 2. Note that similar results for the BSA have also been obtained using heavier targets (D, Ne) [10].

The expected predominant $\cos\phi$ behavior of the BCA (see Eqn. 2) has also been observed at HERMES [11]. The right panel of Fig. 2 shows the $\cos\phi$ amplitudes of the BCA on deuterium and hydrogen as a function of $-t$ which are derived from a fit to the BCA in each $-t$ bin [12]. For both targets, the signal only becomes sizeable for larger values of $-t$. While their slightly different behavior at large $-t$ values can be due to incoherent scattering

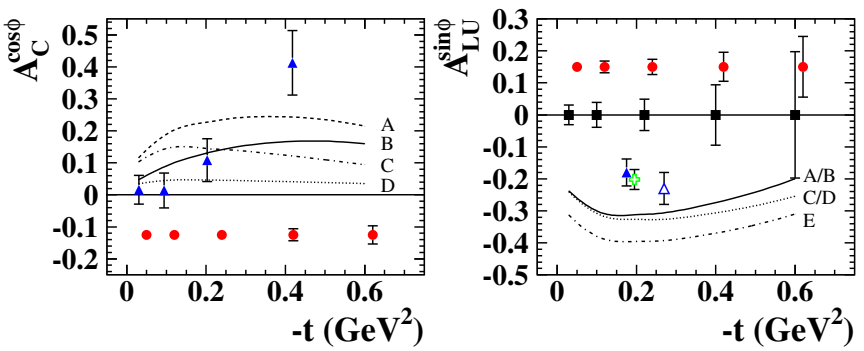

Figure 3. The $\cos\phi$ amplitude of the BCA (left panel, closed triangles) from HERMES [12] and the $\sin\phi$ amplitude of the BSA (right panel) from the 96/97 HERMES data [13] (open triangle), from the 2000 HERMES data [10] (closed triangle), and from CLAS [14] (open cross) as a function of $-t$. The CLAS result was achieved using an electron beam and is thus multiplied by -1. Statistical and systematic uncertainties are added in quadrature. The parameter sets for the GPD models are given in the table. The predictions from the models A, B, C and D are used for comparison with the BCA (left panel). The BSA is insensitive to the D-term contribution and thus yields the same result for the models A/B and C/D (right panel). See text for explanation on the projections (squares,circles).

on the neutron in the deuteron, the approximately 40% contribution of coherent scattering on the deuteron in the first $-t$ bin does not result in a different asymmetry when compared to the proton target, within the uncertainties.

These results together with the ones on the BSA from the 96/97 data [13] and from the CLAS collaboration [14] are shown in Fig. 3. Note that the smaller average $-t$ value of the 2000 data (see right panel) when compared to the result from the 96/97 data is due to the fact that events with small angles between the virtual and the real photon have been included for the analysis of the 2000 data. The model calculations shown in this plot and in the right panel of Fig. 2 are based on a GPD model described in Refs. [15,16]. Since at small values of x_B (t) the contribution from the CFFs $\tilde{H}_1$ (E_1) to the amplitude $M^{1,1}$ is suppressed (see Eqn. 3), the main contribution to the asymmetries in the kinematic region of HERMES originates from the CFF H_1 and thus it originates from the GPD H. Consequently the theoretical calculations shown in Fig. 2 and Fig. 3 were derived by only varying the model parameters for the GPD H in the underlying code [17]

in order to calculate the asymmetries at the average kinematics of every bin. The model parameters (see table) differ with respect to including or neglecting the so–called D–term [18] in the GPD model and whether the t–dependence of the GPD H is calculated in either the simplest ansatz where the t–dependence factorizes from the t–independent part or in the Regge–motivated ansatz. In addition, the parameters b_{val} and b_{sea} in the profile function [19] have been varied. The BCA data appears to disfavor the model with the non–factorized t-dependence and the contribution from the so–called D–term while all models seem to overshoot the absolute size of the $\sin\phi$ amplitude of the BSA.

The extraction of the kinematic dependences of the BSA for the HERA Run I data on hydrogen (1996-2000) is almost completed, the projected statistical precision is shown in the same figure (squares). The additional statistics expected from a dedicated running on unpolarized hydrogen in the final two years of HERA (2006 – 2007) is also displayed (circles), provided that 1 fb^{-1} with each beam charge can be collected at a beam polarization of 40%. While up to now the BSA has always been measured with a positron beam at HERMES and an electron beam at CLAS, the question arises if there are advantages in having both charges and how to combine the data in the first place. The two beam charges do not only result in a different sign for the asymmetry but also the absolute values will be different. This is due to the fact that the numerator of the BSA does not only contain the (helicity dependent) $\sin\phi$ term from the interference term (see Eqn. 2), but also has a (helicity dependent) $\sin\phi$ contribution from the DVCS squared term in Eqn. 1. Despite the fact that the latter is a higher-twist contribution that is suppressed in comparison to the former, it is likely that it will increase the extracted $\sin\phi$ amplitude for one beam charge and diminish it for the other. Especially since kinematic dependences will be studied, the $\sin\phi$ amplitude of the DVCS squared term will not be negligible compared to the $\sin\phi$ amplitude of the interference term in every given kinematic bin. Thus the *ordinary* BSA (see Eqn. 4) will not give a clean access to the interference term, i.e., to linear combinations of GPDs, but will always be disturbed by a

Model	D–Term	b_{val}	b_{sea}	Ansatz t–dependence
A	Yes	1	∞	Regge
B	No	1	∞	Regge
C	Yes	1	∞	factorized
D	No	1	∞	factorized
E	Yes/No	1	1	factorized

term which is proportional to GPDs squared. In addition, the denominator of the BSA should be dominated by the (helicity independent) BH squared term (see Eqn. 1) when compared to the helicity independent part of the interference term, i.e., the $\cos\phi$ term (see Eqn. 2). However, it is also here likely that this (beam charge dependent) $\cos\phi$ term will alter the *ordinary (charged)* BSA since depending on the beam charge it is added or subtracted to/from the BH squared term.

The solution is to define a new cross section asymmetry, which one might call the *neutral* BSA:

$$A^0_{LU}(\phi) = \frac{(d\overrightarrow{\sigma}^+ + d\overleftarrow{\sigma}^-) - (d\overleftarrow{\sigma}^+ + d\overrightarrow{\sigma}^-)}{(d\overrightarrow{\sigma}^+ + d\overleftarrow{\sigma}^-) + (d\overleftarrow{\sigma}^+ + d\overrightarrow{\sigma}^-)}, \tag{5}$$

Apart from the fact that this asymmetry turns out to be independent of the beam charge (*neutral*), it has the important advantage that its $\sin\phi$ amplitude stems solely from the interference term since the (higher twist) $\sin\phi$ dependence of the DVCS squared term drops out. Thus it gives clean access to linear combinations of GPDs, while differences between the ordinary and the neutral BSA can in principle be used to determine the size of these higher twist contributions. It can be concluded that by using the upcoming HERMES data (see Fig.3) for a measurement of this new neutral BSA, together with a measurement of the BCA, one should be able to put serious constraints on the GPD H.

2.2. *Access to GPDs H and $\widetilde{H}$ via longitudinal target-spin asymmetry*

The longitudinal target-spin asymmetry (LTSA) utilizes an unpolarized (U) beam and a longitudinally polarized (L) target. It is calculated as

$$A_{UL}(\phi) = \frac{1}{< |P_T| >} \frac{(N^{\leftarrow\Leftarrow}(\phi) + N^{\rightarrow\Leftarrow}(\phi)) - (N^{\leftarrow\Rightarrow}(\phi) + N^{\rightarrow\Rightarrow}(\phi))}{(N^{\leftarrow\Leftarrow}(\phi) + N^{\rightarrow\Leftarrow}(\phi)) + (N^{\leftarrow\Rightarrow}(\phi) + N^{\rightarrow\Rightarrow}(\phi))} \tag{6}$$

where P_T is the target polarization and $\leftarrow$ ($\rightarrow$) and $\Leftarrow$ ($\Rightarrow$) denote the orientation of the beam and target spin with respect to the beam direction, respectively. The LTSA should be dominated by a $\sin\phi$ amplitude which eventually is most sensitive to a linear combination of the imaginary parts of H and $\widetilde{H}$. The HERMES results [20] on the $\sin\phi$ and $\sin 2\phi$ amplitudes of the LTSA on the proton and on the deuteron as a function of $-t$ are shown in Fig. 4 for the exclusive sample. While both deuteron amplitudes are slightly negative but essentially compatible with zero, it comes as a surprise that the $\sin 2\phi$ amplitude on the proton is not suppressed with respect to

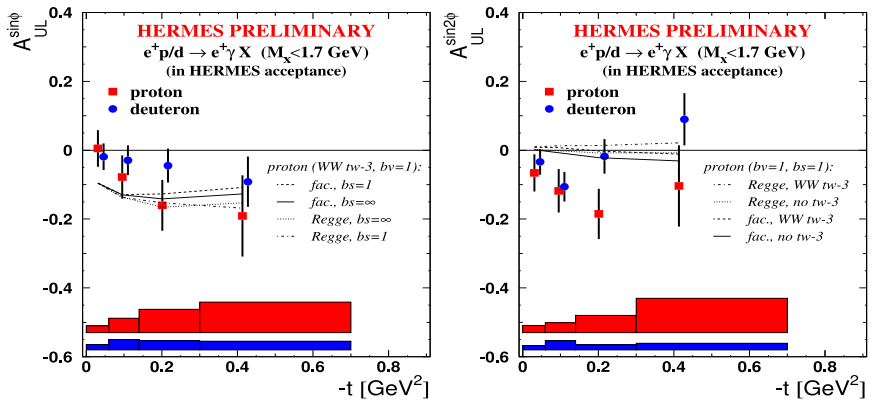

Figure 4. The $\sin\phi$ and the $\sin 2\phi$ amplitude of the longitudinal target-spin asymmetry on hydrogen and deuterium as a function of $-t$ [20].

the non-zero leading-twist $\sin\phi$ amplitude. No difference between the two targets can be seen in the first $-t$-bin where an about 40% contribution from coherent processes on the deuteron is expected. The proton and deuteron results are systematically different for both amplitudes of the asymmetry at higher $-t$ bins, which indicates that the asymmetries on protons and neutrons are different. The results of the model calculations shown in the figures are for the proton case. They are achieved in the same way as described above and show little variation when compared to the statistical error of the data. While the model calculations are in agreement with the data for the $\sin\phi$ amplitude, the (twist-3) $\sin 2\phi$ amplitude of the proton is unexpectedly large when compared to the calculations, as already discussed above. It should be noted here that the model only includes the Wandzura-Wilczek part of the twist–3 contribution but not the genuine twist-3 term.

2.3. *Access to GPDs H and E via transverse target-spin asymmetry*

As described above, HERMES will be able to provide sufficient data to largely constrain the GPD H in the kinematic region of HERMES. It is natural to ask to what extent the GPD E can be accessed, which is the other important GPD necessary in order to determine J_q, the total orbital angular momentum of the quarks in the nucleon [2]. For an unpolarized target the contribution from the GPD E is suppressed with respect to H (see Eqn. 3), but this is different for transverse target polarization [9,21]. Using an unpolarized beam (U) and a transversely (T) polarized target,

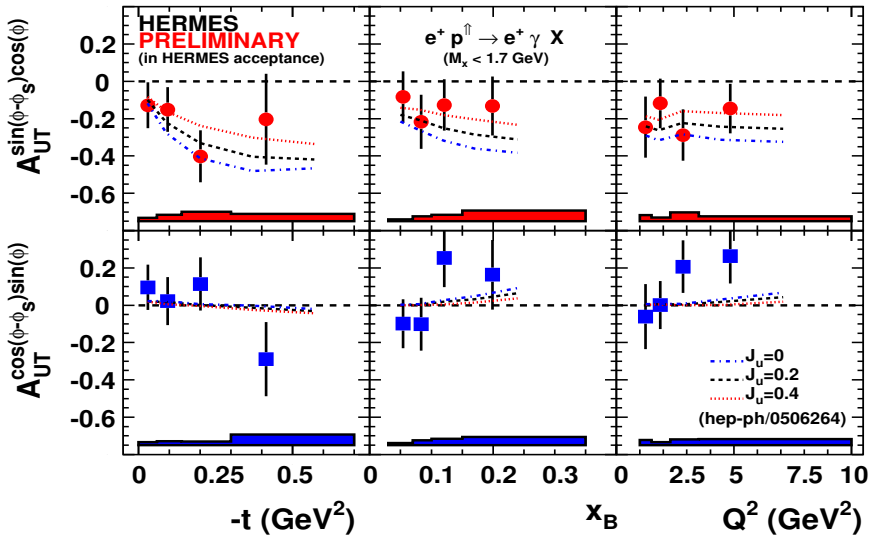

Figure 5. The $\sin(\phi - \phi_S)\cos\phi$ and the $\cos(\phi - \phi_S)\sin\phi$ amplitude of the transverse target-spin asymmetry for the hard electroproduction of photons off the proton as a function of $-t$, x_B and Q^2 in comparison to theoretical predictions from Ref. [22].

the transverse target-spin asymmetry (TTSA) can be written as [22]:

$$A_{UT}(\phi, \phi_s) = \frac{1}{|P_T|} \cdot \frac{d\sigma(\phi, \phi_S) - d\sigma(\phi, \phi_S + \pi)}{d\sigma(\phi, \phi_s) + d\sigma(\phi, \phi_S + \pi)} \propto \tag{7}$$

$$\mathrm{Im}[F_2\mathcal{H}_1 - F_1\mathcal{E}_1]\sin(\phi - \phi_S)\cos\phi + \mathrm{Im}[F_2\widetilde{\mathcal{H}}_1 - F_1\xi\widetilde{\mathcal{E}}_1]\cos(\phi - \phi_S)\sin\phi,$$

where ϕ_s denotes the azimuthal angle of the target polarization vector with respect to the lepton scattering plane.

From 2002 to 2005, HERMES collected data on a transversely polarized hydrogen target. The data set up to 2004 has been analyzed and the results are shown in Fig. 5. They agree with the model calculations [22] shown in the same figure. Since J_u is a parameter in the model for the GPD E, the model calculations confirm that the $\sin(\phi - \phi_s)\cos\phi$ amplitude of the TTSA is sensitive to J_u and thus to E, as expected from Eqn. 7. The calculations of $A_{UT}^{\cos(\phi-\phi_s)\sin\phi}$ on the other hand are almost insensitive to variations on the input values for the GPD model of E, but can in principle be used in order to access the GPDs $\widetilde{H}$ and $\widetilde{E}$. It is interesting to note that the results of the model calculations are largely insensitive to all model parameters but J_u. Taking into account that the GPD H and therefore the available theoretical models will be well constrained by the upcoming

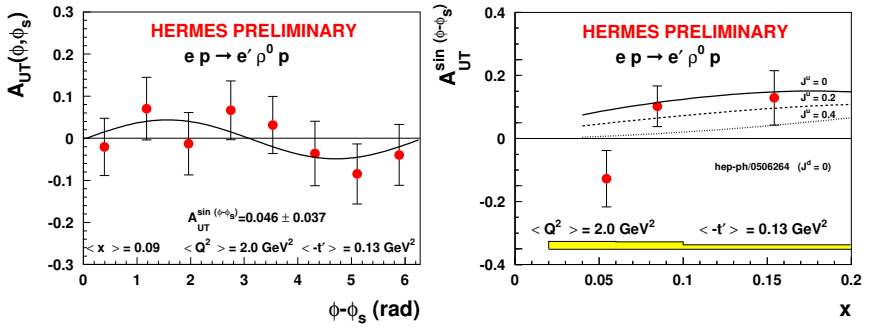

Figure 6. Left panel: Transverse target–spin asymmetry A_{UT} for the hard electroproduction of ρ^0 mesons off the proton as a function of the angle $\phi - \phi_S$. Right panel: The $\sin(\phi - \phi_S)$ amplitude of the transverse target-spin asymmetry as a function of x_B in comparison to model calculations from Ref. [22].

HERMES data, and that the data shown here is less than half of the data taken on the transversely polarized hydrogen target, a model-dependent extraction of J_u with a reasonable precision seems to be possible.

3. Access to GPDs H and E via exclusive ρ^0 production

Besides the TTSA in DVCS, the only other known reaction to access the GPD E on a proton target is the exclusive electroproduction of ρ^0 vector-mesons, $e\,p \to e\,p\,\rho^0$, with the initial proton being transversely polarized. The TTSA is defined as

$$A_{UT}(\phi - \phi_S) = \frac{d\sigma(\phi - \phi_S) - d\sigma(\phi - \phi_S + \pi)}{d\sigma(\phi - \phi_S) + d\sigma(\phi - \phi_S + \pi)} = A_{UT}^{\sin(\phi-\phi_S)} \cdot \sin(\phi - \phi_S). \tag{8}$$

In a strong simplification $A_{UT}^{\sin(\phi-\phi_S)}$ is proportional to the GPD ratio E/H.

Almost half of the HERMES data taken on transversely polarized hydrogen has been analyzed. Events are selected if they contain exactly one positron with $Q^2 > 1$ GeV^2 and exactly two oppositely charged hadrons. Under the assumption that the two hadrons are pions, the calculated invariant mass of the two hadron system has to be within 0.6 and 1.0 GeV while it has to be above 1.04 GeV if calculated under the assumption that both hadrons are kaons. The exclusivity of the reaction is ensured by requiring the missing energy ΔE of the reaction to be below 0.6 GeV. The TTSA as a function of $\phi - \phi_S$ is shown in the left panel of Fig. 6. The fit shows the expected predominant sinusoidal behavior. The $\sin(\phi - \phi_S)$ amplitude of the TTSA as a function of x_B is shown in the right panel of

the same figure. While the data agrees with the model calculations [22] it has to be noted that the model calculations are for longitudinal photons only, for which factorization is proven. The data on the other hand is not yet separated into its longitudinal and transverse parts, which are approximately of equal size at HERMES kinematics. Thus the sensitivity of this TTSA is smaller than the one in DVCS but might still provide additional constraints.

4. Summary

The full HERMES data set on unpolarized targets in addition to the data already taken on the transversely polarized hydrogen target will allow for a model-dependent extraction of the total angular momentum of the u-quark in the nucleon with reasonable precision.

References

1. D. Müller et al., Fortschr. Phys. **42** (1994) 101.
2. X. Ji, Phys. Rev. Lett. **78** (1997) 610, Phys. Rev. **D55** (1997) 7114.
3. A.V. Radyushkin, Phys. Rev. **D56** (1997) 5524.
4. M. Burkardt, Phys. Rev. **D62** (2000) 071503; Erratum–ibid. **D 66** (2002) 119903.
5. A.V. Belitsky and D. Müller, Nucl. Phys. **A711** (2002) 118.
6. J.P. Ralston and B. Pire, Phys. Rev. **D66** (2002) 111501.
7. HERMES Coll., K. Ackerstaff et al., Nucl. Instr. and Meth. **A417** (1998) 230.
8. M. Diehl et al., Phys. Lett. **B411** (1997) 193.
9. A.V. Belitsky, D. Müller and A. Kirchner, Nucl. Phys. **B629** (2002) 323.
10. HERMES Coll., F. Ellinghaus, Proc. of the 15th Intern. Spin Physics Symposium, Upton, New York, AIP Conf. Proc. **675** (2002) 303, hep-ex/0212019.
11. HERMES Coll., F. Ellinghaus, Nucl. Phys. **A711** (2002) 171.
12. F. Ellinghaus for the H1, ZEUS and HERMES Coll., hep-ex/0410094.
13. HERMES Coll., A. Airapetian et al., Phys. Rev. Lett. **87** (2001) 182001.
14. CLAS Coll., S. Stepanyan et al., Phys. Rev. Lett. **87** (2001) 182002.
15. M. Vanderhaeghen, P.A.M. Guichon and M. Guidal, Phys. Rev. **D60** (1999) 094017.
16. K. Goeke, M.V. Polyakov and M. Vanderhaeghen, Prog. Part. Nucl. Phys. **47** (2001) 401.
17. M. Vanderhaeghen, Private Communication, 2001.
18. M.V. Polyakov and C. Weiss, Phys. Rev. **D60** (1999) 114017.
19. I.V. Musatov and A.V. Radyushkin, Phys. Rev. **D61** (2000) 074027.
20. HERMES Coll., M. Kopytin, Proc. of the 13th Intern. Workshop on Deep Inelastic Scattering, Madison, Wisconsin, AIP Conf. Proc. **792** (2005) 424.
21. M. Diehl, Phys. Rept. **388** (2003) 41.
22. F. Ellinghaus, W.-D. Nowak, A.V. Vinnikov and Z. Ye, hep-ph/0506264.